Myoblasts and Embryonic Stem Cells Differentially Engraft in a Mouse Model of Genetic Dilated Cardiomyopathy

Cyril Catelain[1–5], Stéphanie Riveron[1–5], Aurélie Papadopoulos[1–5], Nathalie Mougenot[5,6], Adeline Jacquet[5,6], Karine Vauchez[1–5], Erica Yada[1–5], Michel Pucéat[7], Marc Fiszman[1–5], Gillian Butler-Browne[1–5], Gisèle Bonne[1–5,8] and Jean-Thomas Vilquin[1–5]

[1]UPMC UM 76, Groupe Hospitalier Pitié-Salpêtrière, Paris, France; [2]INSERM U974, Groupe Hospitalier Pitié-Salpêtrière, Paris, France; [3]CNRS UMR 7215, Groupe Hospitalier Pitié-Salpêtrière, Paris, France; [4]Association Institute of Myology, Groupe Hospitalier Pitié-Salpêtrière, Paris, France; [5]Groupe Hospitalier Pitié-Salpêtrière, Paris, France; [6]INSERM UMRS 956, UPMC, Team Stem Cell and Cardiogenesis, Evry, France; [7]INSERM UMR 633, Team Stem Cell and Cardiogenesis, Evry, France; [8]AP-HP, Groupe Hospitalier Pitié-Salpêtrière, U.F. Cardiogénétique et Myogénétique, Service de Biochimie Métabolique, Paris, France.

The functional and architectural benefits of embryonic stem cells (ESC) and myoblasts (Mb) transplantations into infarcted myocardium have been investigated extensively. Whereas ESC repopulated fibrotic areas and contributed to myocardial regeneration, Mb exerted their effects through paracrine secretions and scar remodeling. This therapeutic perspective, however, has been less explored in the setting of nonischemic dilated cardiomyopathies (DCMs). Our aim was to compare the integration and functional efficacy of ESC committed to cardiac fate by bone morphogenic protein 2 (BMP-2) pretreatment and Mb used as *gold standard* following their transplantation into the myocardium of a mouse model of laminopathy exhibiting a progressive and lethal DCM. After 4 and 8 weeks of transplantation, stabilization was observed in Mb-transplanted mice (P = 0.008) but not in groups of ESC-transplanted or medium-injected animals, where the left ventricular fractional shortening (LVFS) decreased by 32 ± 8% and 41 ± 8% respectively. Engrafted differentiated cells were consistently detected in myocardia of mice receiving Mb, whereas few or no cells were detected in the hearts of mice receiving ESC, except in two cases where teratomas were formed. These data suggest that committed ESC fail to integrate in DCM where scar tissue is absent to provide the appropriate niche, whereas the functional benefits of Mb transplantation might extend to nonischemic cardiomyopathy.

Received 19 July 2012; accepted 2 January 2013; advance online publication 26 February 2013. doi:10.1038/mt.2013.15

Cell therapies are progressively emerging as promising tools for the treatment of heart failure. In an attempt to achieve cardiac cell-based replacement therapy in the setting of postischemic cardiomyopathies (ICM), a variety of adult cell types have been tested up to preclinical stages in small and large animal models, including skeletal myoblasts (Mb), muscle-derived stem cells, adipose-derived stem cells, bone marrow mononuclear cells, hematopoietic stem cells, circulating endothelial progenitors, mesenchymal stem cells, smooth muscle cells, cardiac stem cells, and most of these approaches have demonstrated some degree of efficacy.[1–7] Except for some specific populations of cardiac stem cells, most categories of adult stem cells show partial or complete inability to produce *bona fide* cardiomyocytes and to participate to true myocardial tissue formation, with respect to homogeneity of electrical conduction.[8] Their functional benefits would be linked, essentially, to the mechanical strengthening of the scar tissue, and/or to the promotion of myocardial cell survival through paracrine synthesis of trophic factors and/or improved local angiogenesis.[1,4,7–11] Indeed, phase II randomized clinical trials developed using adult stem cells have provided encouraging but still limited results.[12,13] However, the applicability and therapeutic relevance of cell therapies remain under-explored for nonischemic heart failure (dilated cardiomyopathy (DCM), myocarditis), probably due to the progressive nature of the disease and extension of fibrotic remodeling, which make the targeting of a specific area more difficult than when considering a delineated scar formed upon myocardial infarction. A few preclinical studies have been carried out using Mb,[14,15] smooth muscle cells or ventricular heart cells[16] in cardiomyopathic hamsters, or mesenchymal stem cells,[17] mixed mesenchymal stem cells and Mb,[18] or bone marrow cells in rat models of DCM.[19] Among those studies, Mb seem to have the best potential of integration in the dilated myocardium, and represent a "gold standard" for cell-based therapy, although these cells are not able to differentiate into cardiomyocyte lineage.

In contrast, embryonic stem cells (ESC) are pluripotent and can be readily committed towards the cardiogenic lineage *in vitro*. There is also increasing evidence that cardiac-committed ESC can engraft into the scar tissue within the infarcted myocardium and differentiate into cardiomyocytes, thereby operating a regeneration of the myocardium, eliminating fibrotic scar tissue, and promoting

Correspondence: *Jean-Thomas Vilquin, UPMC UM76, INSERM U974, CNRS UMR 7215, AIM, IFR14, Groupe Hospitalier Pitié-Salpêtrière, Bâtiment Babinski, 47 Boulevard de l'Hôpital, 75651 Paris Cedex 13, France. E-mail: jt.vilquin@institut-myologie.org*

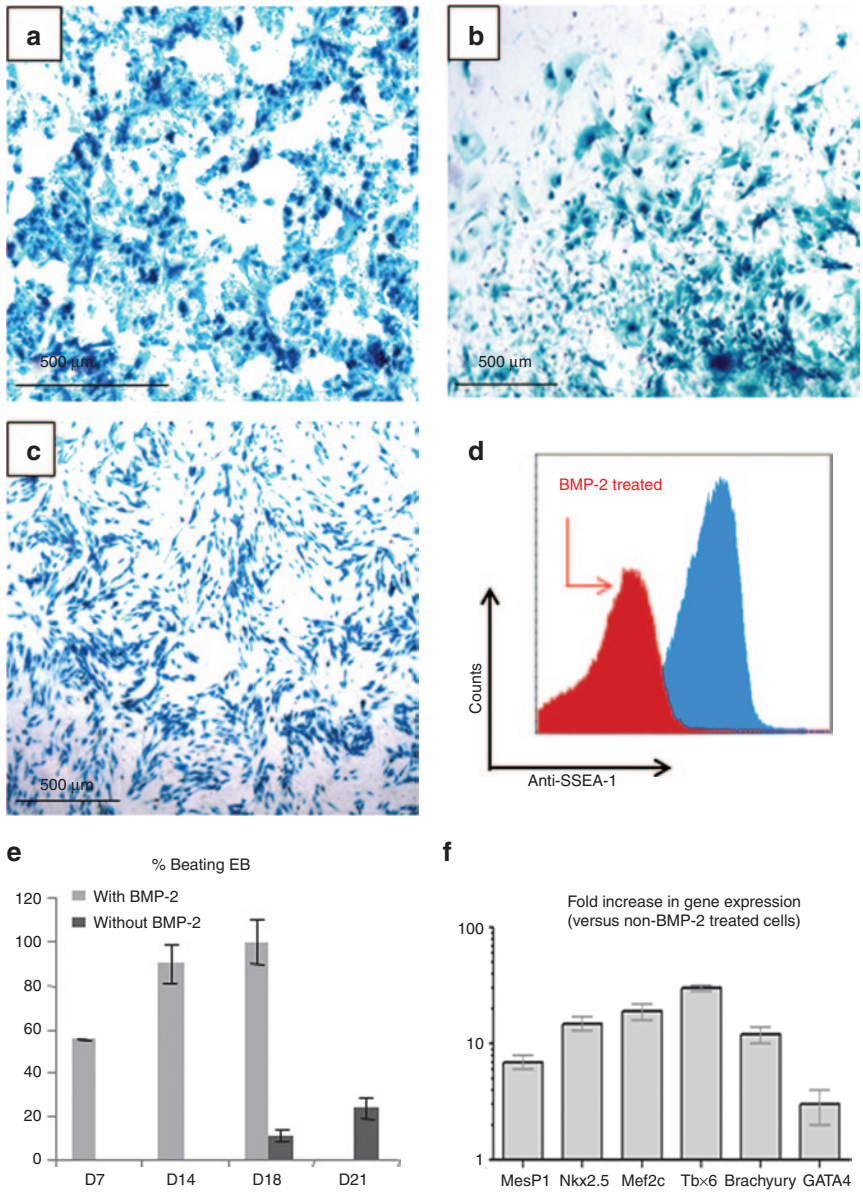

Figure 1 Preparation of murine ESC and Mb expressing (β-Gal and validation of cardiogenic commitment. β-Gal activity was revealed by incubation with X-Gal reagent and visualized by light microscopy in CGR8 ESC (**a**) maintained in a pluripotent state by LIF or (**b**) differentiated *in vitro* in embryonic bodies (EBs), and (**c**) in proliferating D7LNB1 Mb. The commitment of ESC was assessed by flow cytofluorimetry using anti-SSEA-1 staining (**d**). Pretreatment with BMP-2 turned down the expression of SSEA-1 in approximately 65% of the cells (red area), as compared with the level expressed by non-pretreated cells (blue area). (**e**) The numbers of beating EB were compared with or without BMP-2 pretreatment. EBs were scored positively when at least three separate areas of the mesodermal layer were contracting. Data are means ± SEM of four experiments. Upon commitment, (**f**) the expression of cardiac genes was quantified and presented relatively to that of non-pretreated cells. ESC, embryonic stem cells; Mb, myoblasts; LIF, leukemia inhibitory factor.

sustained improvement of left ventricular function.[7,8,11,20–26] This confers the potential ability to rebuild true cardiac tissue, to replenish areas that have been depopulated following ischemic accidents or the progression of fibrosis.[8] In contrast, this positive benefit is limited by the formation of teratomas[27] or if too many cells are in uncommitted state at the time of injection.[24]

In the present study, we have compared the integration and functional efficacy of the CGR8 line of murine ESC with the D7LNB1 line of murine Mb, in the myocardium of *Lmna*$^{H222P/H222P}$ mice. This genetic model of laminopathy reproduces a human missense mutation in the *Lamin A/C* gene causing Emery-Dreifuss muscular dystrophy. This model exhibits a rapidly progressive and lethal DCM,[28] showing pathophysiological evolution and conduction defects comparable to the human situation. Of note, these animals are immunocompetent.

The CGR8 cell line of ESC was chosen because it can be grown feeder-free, and it is efficiently committed toward cardiogenic differentiation *in vitro* upon treatment with bone morphogenic protein 2 (BMP-2),[23,24,29,30] a treatment that indirectly lowers the risk of teratoma formation *in vivo* by decreasing the proportion of pluripotent cells.[24,27] The committed CGR8 cells, whether selected or not, have been previously shown to efficiently improve cardiac

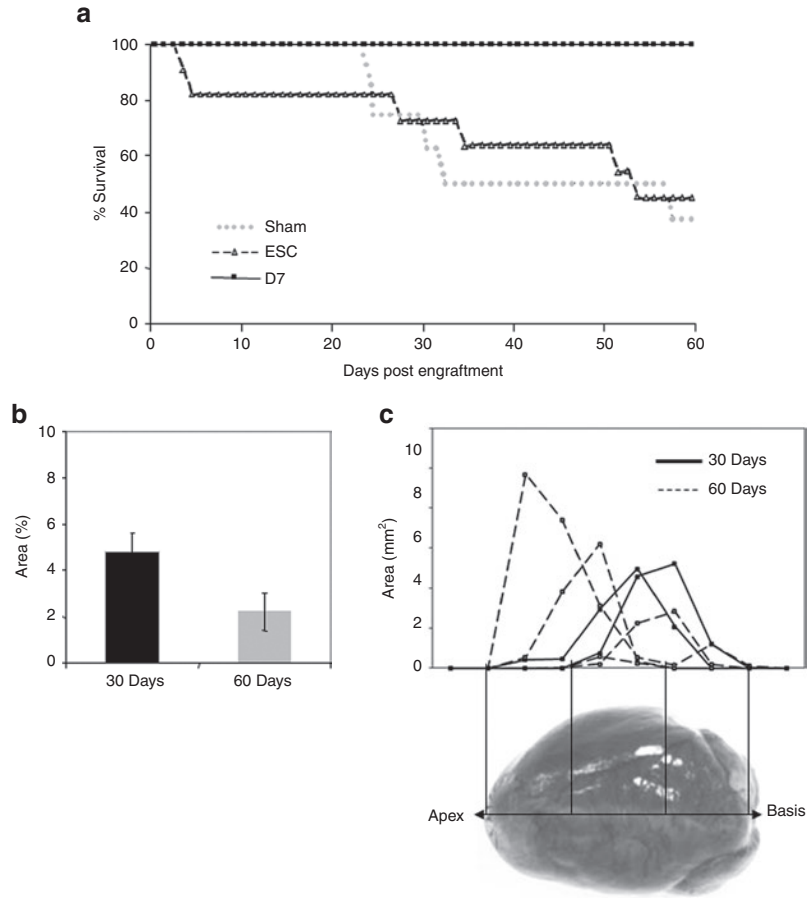

Figure 2 Long-term survey of mice and of engrafted areas after transplantation. Age- and LVFS-matched, female *Lmna*$^{H222P/H222P}$ mice (n = 26) were randomized into three groups receiving no cell implantation (Sham, n = 8), ESC (ESC, n = 11) or D7LNB1 cells (D7, n = 7, two mice have been killed at 30 days postengraftment). (**a**) Survival follow-up is represented by cumulative survival curves over a 2-months course. (**b**) Successive heart sections, representing the whole myocardium from apex to basis, were stained using X-Gal reagent, and means ± SEM of percentages of positive surfaces over the total surface of sections are represented. If any, the surface occupied by ESC was not sufficient for being quantified, and the graph pertains to mice injected with D7LNB1 mice. (**c**) The calculation of the positive areas delineated the anatomic localization of D7 Mb 30 (n = 2) and 60 (n = 4) days after myocardial injection. Most cell clusters were concentrated at injection sites in the septum or in the left ventricular free wall. ESC, embryonic stem cells; LVFS, left ventricular fractional shortening.

function following injection into the scar tissue in animal models of postischemic heart failure.[7,8,23–25] The time window for the addition of BMP-2 is of crucial importance,[30] therefore we pretreated CGR8 ESC for a short period of time, and we designed the experiments using limited amounts of cells to reach a compromise between myocardial differentiation and risk of teratoma formation (3×10^5 per heart, at four different sites).

The Mb have been assayed, in the present study, as a gold standard for validating the injection procedure, the efficacy of the immunosuppression regimen, the natural evolution of the implanted cells, the immunohistological procedures. Comparisons between Mb and ESC in murine models of postischemic heart failure have pinpointed important intrinsic differences in the efficacies and persistence of these two cell types, which now deserve a comparison in a DCM model.[11] The D7 Mb cell line was originally derived from the *dy/dy* mouse model of laminin-2 deficient congenital muscular dystrophy.[31] It was engineered to express β-Galactosidase (β-Gal) constitutively and named D7LNB1. It showed no modification in its ability to form myotubes *in vitro* and *in vivo*. In addition, unlike C2 or G8 murine Mb, D7LNB1 Mb cell line did not produce carcinomas *in vivo*.[32] CGR8 ESC and D7 Mb originate from close parental strains of 129 mice derived from the same animals in the 1970's (129P/Ola background for ESC, 129/ReJ background for D7), and they share identical markers.[33] To avoid immune rejection triggered by murine ESC[34] or Mb[35] further expressing β-Gal in allogenic contexts, recipient mice were immunosuppressed using Tacrolimus.[36] We compared the engraftment of committed ESC and D7LNB1 Mb in terms of functional benefits and fate of engrafted cells *in vivo*. Our results suggest that cardiac-committed ESC failed to engraft into the dilated myocardium of the *Lmna*$^{H222P/H222P}$ mice model, whereas Mb have a higher transplantation efficiency and greater functional improvement of cardiac function in this genetic model of dilated heart failure.

RESULTS

Profiles of CGR8 ESC and D7LNB1 Mb in culture

Murine ESC from CGR8 line and the murine D7LNB1 Mb line were engineered to express the reporter β-Gal transgene to follow their fate within recipient heart tissue. These ESC and derived embryoid bodies (EBs), and D7LNB1 Mb cell lines all expressed

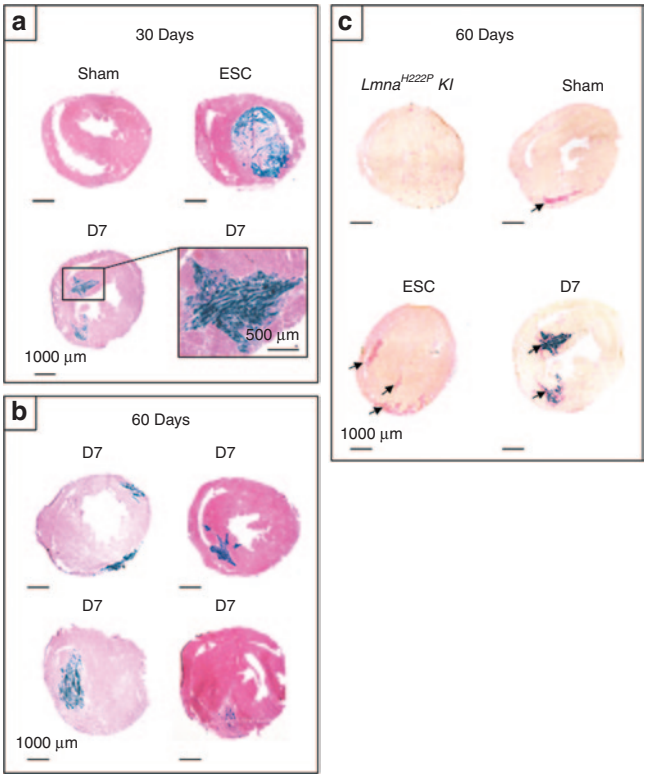

Figure 3 Comparative myocardial histology 1 and 2 months after injection. Transversal heart sections of *Lmna*$^{H222P/H222P}$ mice injected with ESC, D7, or placebo were stained with X-Gal reagent, followed by (**a**,**b**) H&E or (**c**) Sirius Red. Clusters of β-Gal–positive cells were observed at variable localizations (apex, ventricular wall, septum), thus reflecting the multisite injection methodology, in all but one animal of the *Lmna*-D7 group, but not in animals of *Lmna*-Sham group nor of *Lmna*-ESC group excepted in two animals where they formed (**a**) teratomas. Because the cells were injected in beating hearts (approximately 500 beats per minute), the exact trajectory and final implantation may vary from one mouse to the other, as illustrated in **b**, where each section is obtained from a single animal. Large and irregular tracks of collagen depositions were observed (arrows) in each myocardium having received cells or placebo, but not in noninjected *Lmna* animals, and resembled (**c**) needle injection trajectories. ESC, embryonic stem cells.

β-Gal activity *in vitro* (**Figure 1a–c**), as demonstrated by the blue staining following incubation in X-Gal reagent. ESC were committed to a cardiac fate using BMP-2 pretreatment. The BMP-2 incubation decreased the proportion of cells expressing the CD15 (stage-specific embryonic antigen 1, SSEA-1) marker, indicating the enrichment in cardiac-committed cells by 60 to 65% (**Figure 1d**). The pretreatment also promoted the differentiation of EBs *in vitro*. By 14 days (from day 7 to day 21), beating clusters appeared within all of the EBs prepared from BMP-2-primed ESC, while only 20% of EBs prepared from unprimed ESC contained such beating bodies (**Figure 1e**). The incubation also promoted several-fold increases in expression of cardiac markers as evaluated by reverse transcription PCR (**Figure 1f**).

Long-term survey of mice and cell engraftment after transplantation

Female *Lmna*$^{H222P/H222P}$ mice develop abnormal phenotypes more progressively than males and present longer life spans, although

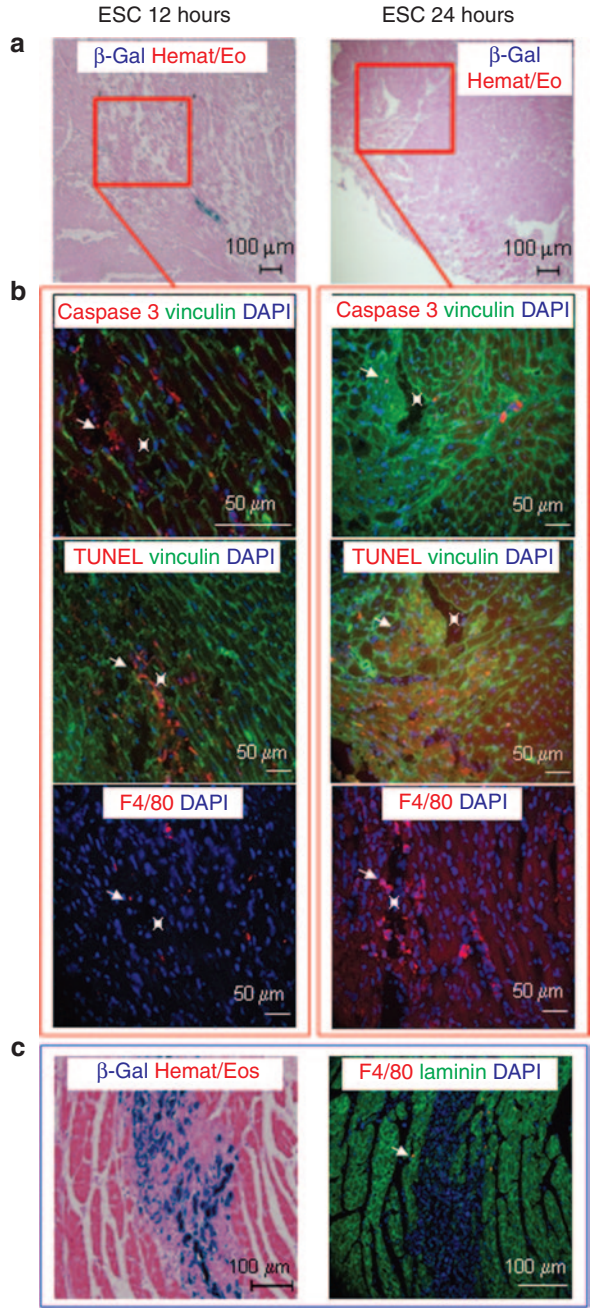

Figure 4 Short-term assessment of cell implantation. Transversal sections of *Lmna*$^{H222P/H222P}$ mice injected with (**a**,**b**) ESC or (**c**) D7 were stained (**a**,**b**) 12 hours, 24 hours or (**c**) 72 hours later for β-Gal activity revelation with X-Gal reagent, for recognition of TUNEL activity, for expression of active caspase 3, or for the presence of infiltrating macrophages (in red). Cardiac cells were delineated by staining of (**b**) vinculin (in green). (**a**) Small clusters of β-Gal–positive ESC were observed at short times after injection only, whereas (**c**) large areas of β-Gal–positive D7LNB1 Mb were observed at 72 hours. (**b**) ESC presented features of apoptosis and necrosis and their injection sites were invaded by macrophages, whereas (**c**) inflammation was very limited at the sites of D7 injections. ESC, embryonic stem cells; Mb, myoblasts.

reduced when compared with the wild-type mice. Then female mice have been used throughout this long-term study. Twenty-six animals of matched ages (177 ± 21 day old) and left ventricular fractional shortening (LVFS; 39 ± 4%) were randomized into

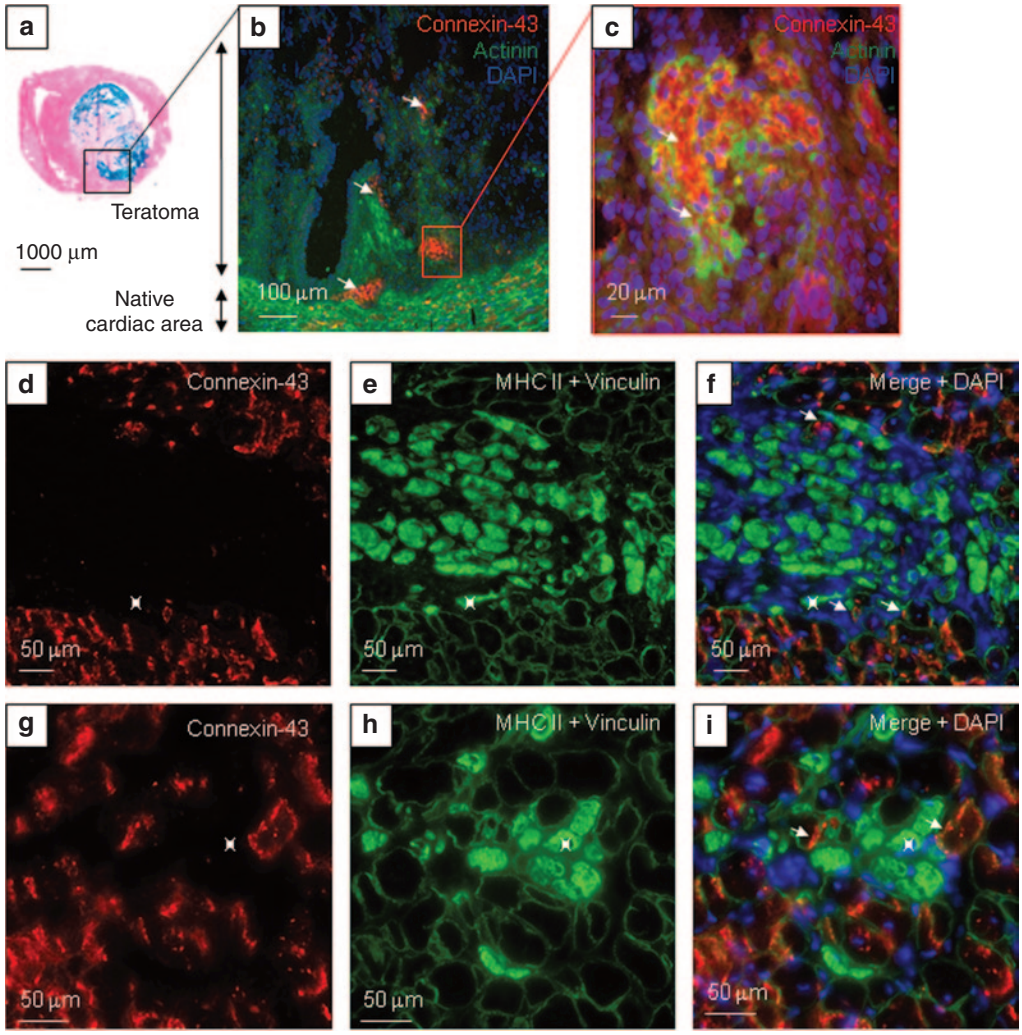

Figure 5 Cardiac differentiation profile of committed ESC and Mb upon transplantation. In the (**a**–**c**) *Lmna*-ESC group, engrafted ESC persisted in two mice as (**a**) teratomas (stained in blue with X-Gal reagent). Cx43 (red), α-actinin (green), and DAPI (blue) expressions were observed (arrows) in the native cardiac tissue, and in clusters within the tumoral mass. In the (**d**–**i**) *Lmna*-D7 group, Cx43 labeling (red) was observed in the native cardiac tissue, and at the periphery of the newly developed skeletal myogenic tissue stained for MHC II (inside of fibers in green). (**e**,**f**,**h**,**i**, green) Cardiac and skeletal muscle cells were delineated by vinculin staining. (**f**,**i**) Skeletal myogenic myotubes or fibers (green, *) did not express cardiac antigens. DAPI, 4′,6-diamidino-2-phenylindole, dihydrochloride; ESC, embryonic stem cells; Mb, myoblasts; MHC, myosin heavy chains.

three groups receiving no cell implantation (*Lmna*-Sham, $n = 8$), ESC (*Lmna*-ESC, $n = 11$) or D7LNB1 cells (*Lmna*-D7, $n = 7$) to evaluate cell-based therapy during a 2-month period. Upon small left thoracotomy, 3.10^5 cells or medium were injected at four sites on the anterior-lateral wall of the left ventricle. To avoid rejection of β-Gal-expressing CGR8 ESC and D7LNB1 cells, all animals were immunosuppressed using Tacrolimus. Survival analysis (**Figure 2**) indicated that all mice of *Lmna*-D7 group survived until the end of the study compared with the *Lmna*-ESC and *Lmna*-Sham groups, because 5 out of the 8 mice from the *Lmna*-Sham group and 6 out of the 11 mice from the *Lmna*-ESC group showed a severe deterioration and had to be killed prematurely. It should be noted that two mice in the *Lmna*-ESC group developed a lethal thoracic teratoma within the first month. Nevertheless, none of the animals in the *Lmna*-D7 group showed any deterioration during the same period (**Figure 2a**). All surviving animals were killed at the end of the 2-month period, however, because animals of *Lmna*-Sham and *Lmna*-ESC groups had to be killed prematurely, we also killed two of the mice in the *Lmna*-D7 group at 1 month to compare the fate of injected cells.

X-Gal staining revealed positive engraftment in cell-injected groups at 1 and 2 months: β-Gal–positive cells were found in 2 out of 11 animals of the *Lmna*-ESC group (*i.e.,* 18%) and in 6 out of 7 animals of the *Lmna*-D7 group (*i.e.,* 86%). D7LNB1 cells were observed in all but one injected heart, thus validating the injection procedure, and the robustness of the immunosuppressive protocol. In the *Lmna*-D7 group, the surfaces occupied by the transplanted cells identified by X-Gal staining were estimated by morphometric analysis and reached 4.8 ± 0.8% of total myocardial surface in certain sections 1 month after transplantation. Interestingly, although the number of animals was small and did not allow statistical comparisons, we observed a trend towards a decrease in surface occupied by transplanted cells with time, because β-Gal–positive cells represented only 2.2 ± 1.4% of the

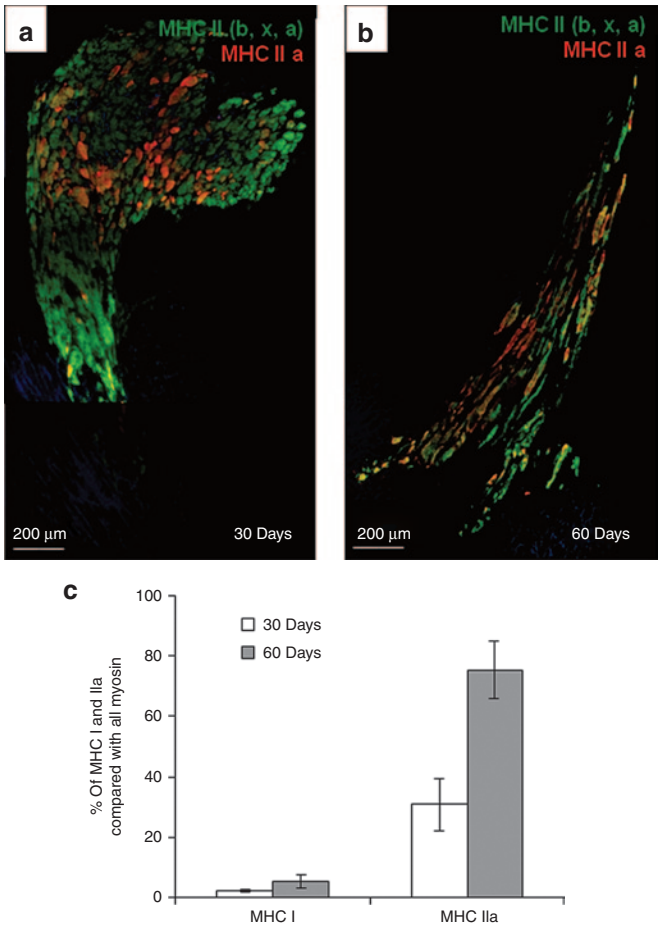

Figure 6 Myogenic transition of transplanted D7Mb. (**a**) Thirty days and (**b**) 60 days after cell injection, clusters of skeletal muscle fibers express the fast isoform of MHC II (green), some of which expressing MHC IIa (red), whereas the cardiac tissue is not labeled. Nuclei are stained in blue. **a** and **b** were reconstructed by juxtaposition of low magnification images. (**c**) The counting of individual fibers indicated a transition with time towards fast oxidative isoform. MHC, myosin heavy chains.

total section surface 2 months after transplantation (**Figure 2b**, $n = 4$). These clusters were observed at variable localizations (apex, ventricular wall, septum) probably reflecting the multisite injection methodology. The most substantial engraftment was generally localized in the septum (**Figure 2c**). The injected D7LNB1 cells formed small β-Gal–positive structures resembling myotubes or small skeletal muscle fibers (**Figure 3a,b**) and expressing myosin heavy chains (MHC) isoforms (see below).

In contrast, the structures which were observed in the two animals of the *Lmna*-ESC group presented a very different nature. Indeed, β-Gal–positive cells in this group corresponded to the development of thoracic and/or intracardiac teratomas. No β-Gal–positive cells could be found in 9 out of 11 of the *Lmna*-ESC group which did not develop teratomas and survived for the duration of the experiment, 1 or 2 months after implantation.

Sirius Red staining illustrated the extent of fibrosis within the hearts of these models. Apart from interstitial fibrosis, which constitutes a hallmark of remodeling in such animal models with DCMs, larger and irregular tracks of collagen depositions were observed in all hearts and evoked the needle injection trajectories (**Figure 4c**). Such collagen depositions were also observed surrounding the areas occupied by D7LNB1 β-Gal–positive cells in the group of *Lmna*-D7 animals.

Short-term engraftment of ESC

As reported above, important differences exist between the fates of D7LNB1 Mb and ESC 1 and 2 months after transplantation. Also, the implantation yield of ESC in our mouse model is strikingly different from that reported in mouse models of postischemic heart failure. These observations may not be predictive of the final functional efficacy, because cells may exert their effects through different mechanisms and kinetics. However, such differences prompted the examinations of the short-term fate of ESC. $Lmna^{H222P}$ mice were injected with ESC or D7LNB1 Mb and killed 12, 24, and 72 hours later (ESC) or at 72 hours later (D7LNB1). While β-Gal activity associated to the presence of ESC can be readily observed 12 hours after injection (**Figure 4a**), very few cells, if any, were observed at 24 hours (**Figure 4a**) and 72 hours after injection (not shown). In parallel, D7LNB1 cells occupied much larger areas 72 hours after injection (**Figure 4c**). These results suggested that at short times after injection D7LNB1 cells showed a better survival and implantation than ESC. We then tried to determine the causes of this decrease in survival using caspase 3 staining to detect cellular necrosis, TUNEL methodology to visualize the extent of apoptosis, and macrophage staining to illustrate the extent of nonspecific inflammation. Both necrosis and apoptosis were activated upon injection of ESC (**Figure 4b**), and the tissue also became infiltrated by macrophages and neutrophils. These cells may participate to the removal of cellular debris, and to the regeneration of myocardial tissue harmed by the needle puncture.

Cardiac differentiation profile of committed ESC upon transplantation

As indicated above, β-Gal–positive ESC were not observed in 9 out of 11 animals. In the two animals, where β-Gal–positive ESC were observed, the formation of cardio-thoracic teratomas precluded their survival. Within these cellular masses (**Figure 5a**), we observed small clusters of cells expressing cardiac-specific antigens such as connexin-43 (Cx43) and α-actinin (**Figure 5b–c**). This indicated that some ESC have acquired a cardiogenic phenotype, upon development within the teratoma tissue.

Myogenic differentiation of transplanted D7LNB1 cells

As expected, D7LNB1 Mb did not promote teratoma formation upon implantation. They also did not express Cx43 and α-actinin, further confirming that Mb cells do not transdifferentiate into cardiac tissue upon integration (**Figure 5d,g**). By contrast, and as a positive control, Cx43 labeling was observed at the periphery of the implantation area surrounding this new myogenic tissue.

The nature of structures formed by D7LNB1 cells was further investigated using antibodies directed against specific isoforms of MHC, that are classified by their velocity of shortening in this following order: MHC I slow twitch oxidative (SO-MHC I), MHC IIa fast-twitch oxidative glycolytic (FOG-MHC IIa) and the MHC IIx and IIb fast-twitch glycolytic (FG-MHC IIx/b). Hybrid

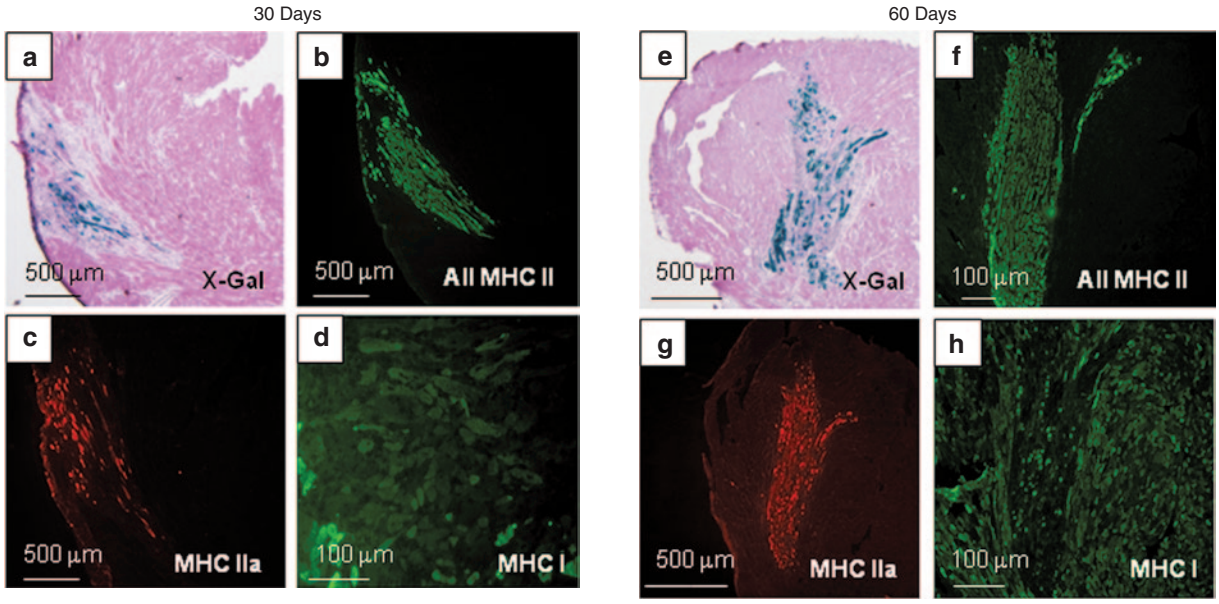

Figure 7 Transition of skeletal muscle tissue from fast to slow phenotypes. (**a**,**e**, blue) X-Gal reagent and (**b**,**f**) MHC II isoform labeling identified clusters of engrafted fibers. Total fast twitch (**b**,**f**) MHC II and more specifically (**c**,**g**) MHC IIa fibers predominated over slow twitch (**d**,**h**) MHC I fibers 30 and 60 days after cell injection. MHC, myosin heavy chains.

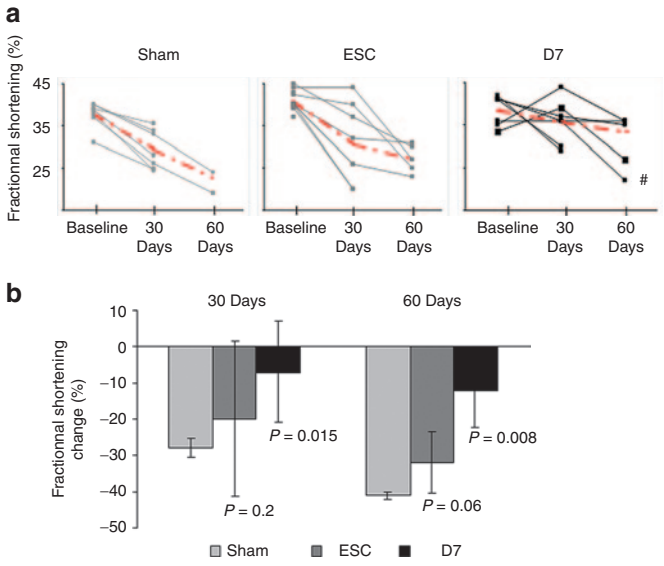

Figure 8 Benefit of cell therapy on contractile function. Cardiac function was evaluated by echocardiography and plotted individually (**a**) per animal (the red bars illustrate the means in each group), or globally (**b**) per group. Fractional shortenings were measured immediately before transplantation (baseline) and 30 and 60 days after injection with either culture medium (Sham, $n = 8$), ESC (ESC, $n = 11$), or D7Mb (D7, $n = 7$). The animal labeled by the dash (#) was the only one found negative for X-Gal staining and was not included in calculations of means. In **b**, fractional shortening change was normalized by fractional shortening baseline in the respective group. ESC, embryonic stem cells; Mb, myoblasts.

fibers expressing FOG-MHC IIa and FG-MHC IIx/b represent a subpopulation able to adapt quickly to functional changes.[37] Fast-twitch isoforms are expressed by skeletal muscle structures but not by adult cardiomyocytes. We first observed that, within the implanted areas, the myogenic structures (myotubes, small muscle fibers) expressed one or several MHC isoforms, at least MHC II (Figure 5e,5f). We then calculated by morphometric analysis the surface occupied by myogenic structures as a function of isoform expressed, and we observed a progressive transition between isoform. Initially, the FG-MHC IIx/b fibers occupied 67.1 ± 9% of the grafted areas 1 month after injection, while the FOG-MHC IIa occupied 30.8 ± 8.5% of total counted engrafted fibers. At the 2-months time point, the estimated surface of cells expressing FOG-MHC IIa increased to 75.4 ± 9.4% ($P = 0.004$) and then replaced FG-MHC IIx/b. The percentage of SO-MHC I fibers increased from about 2.1 ± 0.5% at 1 month up to 5.1 ± 2.6% at 2 months postengraftment ($P = 0.38$, not significant) (Figure 6). These results suggest a transition from a fast to slow phenotype that could occur along the classical sequence of myosin transitions IIb, IIx, IIa, then type I and would confirm previous observations in different animal models,[37,38] proposing a progressive adaptation to the endogenous environment (Figure 7).

Benefit of cell therapy on contractile function

Before transplantation these age-matched animals presented the same baseline echocardiographic values between groups (*Lmna*-Sham, mean LVFS 39 ± 5%; *Lmna*-ESC, mean LVFS 40 ± 4%; *Lmna*-D7, mean LVFS 38 ± 4%), showing an overall significant decrease of LVFS (39 ± 4%), as compared with the wild-type mice (43 ± 1%, age-matched wild-type mice, $n = 12$, $P = 0.005$; data not shown). One month after transplantation, *Lmna*-D7 group showed a stabilization of the LVFS (36 ± 5%) as compared with the *Lmna*-Sham group (29 ± 2%, $P = 0.015$), while the *Lmna*-ESC group (32 ± 9%) showed a similar decrease to that observed in the *Lmna*-Sham group ($P = 0.235$) (Figure 8). Two-month echocardiographic evaluations confirmed the benefits observed in the *Lmna*-D7 group (34 ± 4%) over the *Lmna*-Sham group (23 ± 3%, $P = 0.008$) and the *Lmna*-ESC (27 ± 3%) ($P = 0.06$). Individual

values and the evolution of the values with time are presented in **Figure 8**. Interestingly, in the *Lmna*-D7 group, the only animal showing a functional deterioration was the unique animal in which no D7LNB1 could be identified, *i.e.,* when the cell transplantation failed.

DISCUSSION

The development of cell therapy approaches for the treatment of DCM is conceptually and technically challenging when compared with the situation encountered in chronic or acute ICM. DCM has multiple etiologic origins, idiopathic or genetic;[39] in addition, in contrast to the infarcted heart, the DCM myocardium does not present a clearly delineated area targetable for cell delivery. Although inducing local ischemia has allowed several animal models of ICM to be developed, only a few models are available to investigate therapeutic approaches for DCM. Our group has engineered a transgenic *Lmna*$^{H222P/H222P}$ mouse, which presents a progressive and diffuse cardiomyopathy due to left ventricular dilatation associated with a critical decrease of contractile function.[28] In these animals, the progression of the disease leaves a gap open for assessment of therapeutic approaches.

ESC were long thought not to be recognized by the immune system but recent results have shown that once they differentiate, they may elicit an immune reaction.[40] Regarding Mb, the immunogenicity of these cells in an allogenic context has been established in several models, but efficient immunosuppression with Tacrolimus can preclude rejection.[35,36] Both CGR8 and D7LNB1 cell lines were derived from SV129 parental backgrounds,[33] but they were engineered to express the immunogenic β-Gal protein and they were not injected in a syngeneic context. To avoid immune rejection, *Lmna*$^{H222P/H222P}$ mice were immunosuppressed with Tacrolimus, allowing long-term persistence of allogenic D7LNB1 Mb or CGR8 ESC.

In this study, we have for the first time compared the efficiency of two different types of progenitors in a faithful model of genetic human DCM, in a controlled immunological context, by coupling short- and long-term follow-up of physiological function and histological engraftment. Only one previous study has compared ESC and Mb transplantation in a mouse model of postischemic heart failure, and it pointed out important differences in the mechanisms of implantation as well as the kinetics and persistence of the different cell types, and the final functional benefits of these cell types.[11]

Mb transplantation in DCM

The positive outcomes resulting from Mb transplantation, which are mainly the result of paracrine mechanisms,[9,11] have been demonstrated in several preclinical models of ICM, as well as in clinical trials which unfortunately produced mitigated results.[12] The efficacy of Mb transplantation in DCM has however only been tested in a few models. Their widespread distribution and functional benefits were observed upon intracoronary infusion in a rat model of doxorubicin-induced DCM.[41] In addition, the cotransplantation of autologous Mb and mesenchymal stem cells improved heart function in a rat model of DCM induced by Chagas disease.[18] In a previous study, our group demonstrated stabilization and improvement of cardiac function upon transplantation of autologous Mb in the CHF147 Hamster model of δ-sarcoglycan deficiency with a DCM.[15] Finally, a clinical study limited to one patient presenting with idiopathic DCM reported improved cardiac function and increased incidence of arrythmias upon injection of autologous Mb at the time of mitral valvuloplasty.[42]

In the present study, we used the D7LNB1 cells as our source of Mb for practical and conceptual reasons. Because of their clonal origin, the D7LNB1 cells are purely myogenic, and the preparations do not present the heterogeneity and variability encountered in primary cell cultures. Also, the number of injected cells is easy to standardize and produce, which is not always the case when considering primary cultures of autologous cells extracted from small and fragile animal models. As for the CGR8 ESC, they originate from a parental strain of 129 mice. Finally, even though it is defective in the production of laminin α2 chain, the D7LNB1 cell line successfully engrafts into striated muscles and does not induce the formation of tumors. Our present results confirm and extend the functional benefit produced by Mb transplantation in this transgenic mouse model featuring the human DCM observed in patients with Emery-Dreifuss muscular dystrophy. The engraftment of Mb stabilized and even improved the function of these failing hearts in all of the mice, except for one animal where cell implantation was not successful. As previously observed in the setting of ICM, cardiac markers such as Cx43 or α-actinin never colocalized with MHC- or β-Gal–labeled myotubes, confirming that implanted Mb do not transdifferentiate into cardiac-like tissue, nor fuse or develop electromechanical coupling with resident cardiomyocytes,[43] although both cell types were in close contact within the noninfarcted myocardium. Interestingly, these skeletal muscle fibers also expressed various MHC isoforms. With time, we observed a shift in isoforms expression, suggesting that myotubes may exhibit some degree of plasticity by adapting their phenotype as a function of their environment.[37,38,44] However, unfortunately, this was accompanied by a progressive decline in the surface area occupied by the skeletal muscle tissue, suggesting a progressive attrition.

ESC transplantation in DCM

The differentiation of ESC into the cardiac lineage is a spontaneous feature in nonproliferative conditions that is strongly increased by short BMP-2 treatment.[23,24,30] Such commitment both reduces the proportion of pluripotent and potentially teratogenic cells[24] and prepares the cardiac progenitors to integrate into the cardiac site of implantation that constitutes a specific microenvironment. It has been shown previously that ESC stimulation by BMP-2 committed up to 70% of cells, as assessed by the decrease in the number of cells expressing the mouse pluripotent stem cell marker SSEA-1,[25,29] by the increased formation of beating bodies *in vitro*,[29] and by the increased expression of cardiac markers.[25] The transplantation of ESC precommitted towards a cardiac fate, whether selected or not, in numerous models of ICM, has demonstrated that ESC progeny engraft and survive within ischemic myocardium, which is filled with loose, relatively amorphous tissue constituting a fresh fibrotic scar.[20,22,25,26] Due to ongoing remodeling, scar tissue secretes large amounts of cytokines such as FGF1, FGF2, and TGFβ upon formation,[45,46] that may favor cell survival, proliferation, and migration. In particular, the TGFβ family of

cytokines may promote or sustain cardiomyogenic differentiation and maturation. In these models of ICM, engrafted cells are mainly observed within the scar area, suggesting that transplanted cells cannot easily migrate towards areas of dense, compact myocardium. A few studies have been dedicated to the transplantation of ESC into murine models of DCM. In a mouse model of doxorubicin-induced DCM, the transplantation of ESC selected positively on the Flk1 marker improved cardiac function, and the transplanted cells expressed cardiac markers and formed gap junctions improving cardiac function.[47] In a model of DCM induced by stress load in a K_{ATP} channel-null mutant, the transplantation of ESC stabilized myocardial deterioration and restored contractile performance.[48,49] Intrinsic differences between our model and the two models cited above made the interpretation of outcomes difficult. Indeed, in our genetic model the disease evolves gradually, whereas DCM is induced in a more acute way in the doxorubicin- or stress load-induced models, suggesting different kinetics of degeneration and remodeling. Also, ESC lines and selection modalities were different between studies.

In the field of cell therapy, final beneficial effects may be due to a small initial number of cells which are able to repopulate large portions of tissues. Therefore, the final outcome may not be completely predicted by the initial number of implanted cells. Moreover, in the context of heart failure repair, the long-term persistence of cells is not always mandatory, because some cell types exert their effect through paracrine mechanisms.[9–11] In the present study, only a few BMP-2-stimulated ESC seem to survive after injection, because no persistent engraftment was observed and teratoma formation was observed in two cases. In parallel, the transplantation failed to improve cardiac function. The formation of teratoma is usually correlated with the initial number of injected cells, due to requirement of autocrine factors to maintain the self-renewal of pluripotent cells *in situ* within the differentiated tissue where they are injected. The transplantation of 3.10^5 uncommitted ESC of CGR8 line has been previously proposed as an upper limit to avoid systematic teratoma formation.[24,27] In the present study, we injected 3.10^5 cells pretreated with BMP-2, which should theoretically leave the preparation below this limit because more than 60% of the cells expressed markers of cardiac commitment after treatment. Indeed, we observed invasive teratoma formation in only 2 out of 11 mice. Therefore, it is unlikely that the presence of uncommitted ESC in excessive numbers precluded the differentiation and integration of committed ESC into cardiomyocytes. Interestingly, the only transplanted cells expressing cardiac markers were observed within the teratoma tissue. Taken together, these observations suggest that the disorganized structure of teratoma in association with its specific embryoid environment, may be more favorable to survival and differentiation of ESC than the compact structure of the differentiated heart. Since, we did not observe graft persistency and cardiac differentiation in any of the nine remaining animals not developing a teratoma. Twelve and 24 hours after injection, apoptosis and necrosis (as assessed by caspase and TUNEL stainings) affected large areas of injected ESC, suggesting a high sensitivity of committed ESC to early death mechanisms in such a hostile environment. Variable susceptibilities to death mechanisms presented by different cell types have been documented in other cell transplantation contexts, such as myogenic cell transplantation in animal models of muscular dystrophies.[50] Our results therefore suggest that BMP-2 stimulated ESC cannot integrate within the heart tissue in this mouse model of DCM, in contrast to the promising results observed in models of ICM, whereas Mb used as a *gold standard* can integrate within the myocardium and also stabilize cardiac function in our DCM model.

The contrasting differences between the engraftment efficiencies of Mb and ESC in this nonischemic model of genetically determined global DCM reflect the different intrinsic properties of these two cell types and their differential requirements to achieve survival and integration. Therefore, the prospective developments of ESC usage may include tools promoting cell implantation into the cardiac tissue. Recent studies reported the use of additives, such as injection with biopolymeric scaffolds,[51] or production of engineered tissue. Because of the diffuse nature of the cardiomyopathy, ESC delivery may call for entrapment within large patches fixed in an epicardial position, as proposed in a model of pacing-induced heart failure.[52] Alternatively, survival cocktails[26] could be used in our animal model of DCM.

CONCLUSIONS

The positive result of engrafted Mb should first be taken as an additional proof of principle that transplanted Mb can engraft into a DCM mouse model which faithfully reproduces a human DCM genetically induced, and this confirms the use of Mb as a *gold standard* in preclinical models of heart failure. Second, the present study highlights the need for new tools to improve ESC integration and survival in dilated cardiac tissue. Finally, this study underlines the usefulness of the *Lmna*^{H222P} mouse model of DCM as a tool to investigate pharmacological, molecular and cellular strategies to treat DCM. Specifically, cellular candidates such as cardiac progenitor cells, muscle-derived stem cells, bone marrow-, or blood-borne stem cells may be assessed and compared in such a setting.

MATERIALS AND METHODS

Cell cultures

Growth and commitment of CGR8 ESC line. CGR8 line has been generated from male murine ESC on the 129P2/Ola background.[29] Cells were maintained in undifferentiated state in high glucose (4.5 g/l) BHK21 medium, supplemented with 2 mmol/l L-glutamine, 0.1 mmol/l nonessential amino acids, 1 mmol/l sodium pyruvate, 50 U/ml penicillin-streptomycin (Life Technologies, Carlsbad, CA), 7% fetal calf serum (HyClone; Perbio Science Erembodegem-Aalst, Autostradelaan, Belgium), and 1000 U/l recombinant human leukemia inhibitory factor (Sigma, St Quentin Fallavier, France).

ESC were engineered to express the reporter β-Gal transgene to follow their fate within recipient heart tissue. β-Gal was preferred over a fluorescent reporter to avoid the high fluorescence background developed in murine hearts. Briefly, lentiviral supernatants (CMV.LacZ WPRE lentivirus, kind gift from Véronique Blouin) were used at multiplicity of infection between 5 and 10. On day 3 after transfection, Fluorescein-di-β-D-galactopyranoside (Sigma) was used as a fluorescent substrate to detect β-Gal–positive clones, and Fluorescein-di-β-D-galactopyranoside–positive ESC were selected by flow cytometry using a FACSDiva (Becton Dickinson, Le Pont de Claix, France). Sorted clones were expanded on ESC medium and a unique stock was frozen and used through the *in vivo* experiments.

To commit ESC towards a cardiac lineage, cells were grown for 24 hours in 7% fetal calf serum, 1000 U/l leukemia inhibitory factor, and 2.5 ng/ml BMP-2 (Invitrogen, Cergy-Pontoise, France) before transplantation. The cardiac commitment was assessed using three complementary methodologies, as previously described.[25,29] First, the

percentage of cells downregulating the expression of the embryonic marker SSEA-1 (CD15) was estimated by flow cytofluorimetry.[25] Untreated and pretreated cells were trypsinized and incubated with anti-CD15 conjugated with fluorescein isothyocyanate (1/300, 15 minutes; Becton Dickinson) and analyzed using a FACS Calibur flow cytometer and the Cellquest software (Becton Dickinson). Second, cultures of EBs were performed as previously described[29] from cells pretreated or not with BMP-2, and the proportion of beating bodies was counted at different days after seeding. Third, the relative expression of cardiac genes upon commitment has been assessed using reverse transcription PCR.[25] Total ESC RNA ($n = 6$) was extracted with a kit (Zymo, Orange, CA). After reverse transcription real-time quantitative PCR was performed using Lightcycler and the SYBR green fast start kit (Roche, Meylon, France) with 10 ng cDNA. Data were normalized using β-tubulin as an index of content and a standard concentration curve. Amplification was performed as described,[25] and fluorescence was measured at the end of every extension step. The melting curves identified the specificity of PCR products, further confirmed by gel electrophoresis. Results are presented as a ratio of expression of the gene of interest compared with the expression of the same gene in noncommitted ESC.

D7Mb cell line. The D7 cell line was originally obtained by David Yaffe from the primary culture of an adult 129ReJ dystrophic *dy/dy* mouse[31] and kindly given to our group. The D7LNB1 cell line was derived after retroviral introduction of a β-Gal reporter transgene and selection of a clone expressing the enzyme while keeping a high capacity to differentiate *in vitro*.[32] D7LNB1 Mb were grown in Dulbecco's modified Eagle's medium supplemented with 20% fetal calf serum (Invitrogen).

Animal model. *Lmna*$^{H222P/H222P}$ *KI* mice were generated and genotyped at the central core facility of our institution (Centre d'Expérimentation Fonctionnelle, Hôpital Pitié-Salpétrière, Paris, France) as previously described.[28] All experimental procedures were performed on female age-matched *Lmna*$^{H222P/H222P}$ mice according to the guide for the care and use of laboratory animals published by the NIH (publication No. 85-23, revised 1996).

Cell transplantation and immunosuppression. Cardiac-committed ESC and D7LNB1 Mb were harvested using trypsin-EDTA (0.025%; Invitrogen), suspended in phosphate-buffered saline (PBS) supplemented with 0.5% bovine serum albumin (Sigma) and kept on ice at $7.5.10^6$ cells/ml. Age-and function-matched (177 ± 21 days and 39 ± 4% of LVFS) female *Lmna* mice were randomized to receive 3.10^5 BMP-2-treated-ESC (n = 11, *Lmna*-ESC group), 3.10^5 D7LNB1 Mb (n = 7, *Lmna*-D7 group), or vehicle medium alone (n = 8, *Lmna*-Sham group). Mice were anaesthetized using ketamine (75 mg/kg) and xylazine (15 mg/kg) and ventilated (MiniVent, Type845; Hugo Sachs Elektronik, March-Hugstetten, Germany). Upon small left thoracotomy at the level of the 5th intercostal space, cells or medium were injected at four sites on the anterior-lateral wall of the left ventricle under a total volume of 40 µl, using a Hamilton syringe and a 32G needle. To avoid immune rejection of allogenic, genetically engineered cells, all animals were daily immunosuppressed using Tacrolimus (Fujisawa, Osaka, Japan) at the dose of 2.5 mg/kg.[36]

One set of experiments was dedicated to the short-term outcome of cell transplantation. Six *Lmna* mice were injected with 3.10^5 BMP-2-treated-ESC and killed 12, 24, and 72 hours later, and their hearts processed for histochemical analysis. Two mice were injected with 3.10^5 D7LNB1 Mb and killed 72 hours later, and their hearts processed for histochemical analysis. All animals were immunosuppressed, and functional evaluation was not assessed.

Assessment of cardiac function by echocardiography. Left ventricular dimensions were obtained under light isoflurane anesthesia (0.5% in O_2; Baxter SAS, Maurepas, France) allowing stabilization of heart rhythm (around 500 beats per minute), using echocardiography-Doppler (Vivid 7 Dimension/Vivid 7 PRO; General Electric Medical Systems, GE Vingmed Ultrasound A/S, Horten, Norvege) with a 9–14 MHz probe. The two-dimensionally guided Time Motion mode recording of the left ventricle provided diastolic and systolic septal and posterior wall thicknesses, internal end-diastolic and end-systolic diameters. The fractional shortening measures left ventricle performance and is a ratio calculated from the measurement of the diameter of the left ventricle in contracted then in relaxed states. Each set of measurements was obtained from a same cardiac cycle. At least three sets of measures were obtained from three different cardiac cycles.

Follow-up of cell integration and differentiation ex vivo. According to experimental groups, 12, 24, and 72 hours or 2 months after transplantation, mice were euthanized under general anesthesia. In the course of the study, some mice progressing critically had to be killed earlier, as indicated. Hearts were snap frozen in liquid-nitrogen-cooled isopentane and serial cryosections (7 µm) collected in a transverse orientation from apex to basis.

X-Gal, hematoxylin-eosin, and Sirius Red staining for graft detection. Following a short glutaraldehyde fixation (0.25% in PBS) and two rinses in PBS, the cryosections were incubated overnight with X-Gal reagent (5-bromo-4-chloro-3-indolyl-β-D-galactopyranoside; Boehringer Mannheim, Laval, Quebec, Canada) at room temperature and finally counter-stained with *hematoxylin-eosin* or Sirius Red. The surfaces containing β-Gal–labeled cells and/or presenting fibrotic infiltration stained by Sirius Red were detected using a Nikon Eclipse E600 microscope (Nikon France S.A., Champigny-sur-Marne, France) and measured using NIS-Elements software (Nikon France S.A.), and expressed as a ratio to the total surface of a given cryosection.

Assessment of cell death processes and local infiltration. These processes were explored at early times after injection, *i.e.,* 12, 24, and 72 hours for *Lmna*-ESC mice and 72 hours for *Lmna*-D7 mice. To assess apoptosis, tissue sections were fixed using paraformaldehyde 1% in PBS (10 minutes) then a mixture ethanol/acetic acid (2/1, 5 minutes at −20 °C). Then, the indirect ApopTag Red detection kit (Millipore Bioscience Research Reagents, Billerica, MA) was used according to manufacturer instructions. To assess necrosis, sections were fixed using paraformaldehyde 4% in PBS (10 minutes), triton 0.2% (10 minutes), and goat serum 10% in PBS (30 minutes), then incubated with anti-active caspase 3 (1/200, 2 hours, Becton Dickinson), and revealed using Alexa Fluor 568-conjugated goat antirabbit IgG (H+L; Invitrogen). To assess macrophage infiltration, sections were fixed using acetone (20 minutes, −20 °C), then bovine serum albumin in PBS (10%, 30 minutes), and incubated with F4/80 rat antimouse antibody conjugated to biotin (1/50, overnight at 4 °C, Serotec, Colmar, France). The staining was revealed using streptavidin conjugated to Alexa Fluor 568 (Invitrogen). Negative controls were obtained by omitting primary antibodies. Slides were mounted in Vectashield medium (AbCys, Paris, France). All images were visualized using an axiophot fluorescent microscope (Carl Zeiss, Le Pecq, France) and analyzed using the Metaview image analysis software (Universal Imaging, Downington, PA).

Assessment of cardiac differentiation in Lmna-ESC group. Tissue sections were incubated with cardiac-specific primary antibodies. Anti-Cx43 (Sigma) was incubated (1 hour, 1/100) and revealed using Alexa Fluor 568 labeled goat antirabbit IgG (H+L; Invitrogen). Anti-vinculin and anti-α actinin (Sigma) were incubated (1 hour, 1/100) and revealed using Alexa Fluor 488 goat antimouse IgG1 and IgG2b, respectively (Invitrogen). Slides were mounted and analyzed as above.

Assessment of myogenic differentiation in Lmna-D7 group. Cryosections underwent double immunolabeling to observe differential MHC expression in engrafted area and surrounding heart tissue. Anti-MHC IIa (clone SC71; DSHB, Iowa City, IA) or anti-MHC II (clone My32; Sigma) and anti-MHC I (clone BAD5; DSHB) were incubated (1 hour, 1/100), and revealed using Alexa Fluor 488 or 568 goat antimouse IgG1 and IgG2b (Invitrogen), respectively. Negative controls were obtained in omitting primary antibodies. Slides were mounted in Vectashield. Images were collected as above and assembled when indicated. The numbers of fibers

expressing each type of MHC isoform were counted in four areas, and ratios between fast oxidative/glycolytic MHC IIa fibers and all type II MHC fibers (gathering IIa, IIb, and IIx fibers) were calculated.

Statistical Analyses. All measurements were performed at least three times. Continuous variables were analyzed using Student's *t* test for paired values. The measured values were expressed as mean ± SEM. *P* values of less than 0.05 were considered to be statistically significant.

ACKNOWLEDGMENTS

We thank the Cardiac Progenitors Transatlantic (CaPTAA) network headed by Philippe Menasché (HEGP, Assistance Publique Hopitaux de Paris) and Kenneth Chien (Harvard University) for fruitful discussions, Serban Morosan and members of the animal experimentation center (Pitié-Salpétrière Hospital) for their assistance and care of the mice. We thank Julia Pouly, Bertrand Leobon, and Bruno Pouzet for their expert help in setting the surgical protocol, and Patrick Bruneval for advices in histological assessments (Assistance Publique Hopitaux de Paris). We acknowledge Véronique Blouin (Institut de Recherche Thérapeutique-ITR1-INSERM UMR649, Nantes, France) for the gift of β-Gal lentiviral supernatants, and Yann Lecluse (Institut Gustave Roussy, Villejuif, France) for FACS cell sorting. This work was supported by the Leducq Foundation through the CaPTAA network (C.C., A.P., and S.R.), by the DIM-STEMPOLE from Région Ile-de-France (C.C. and E.Y.), and by the Association Française contre les Myopathies (AFM; S.R., K.V., E.Y.). Our group is supported by the Centre National de la Recherche Scientifique (CNRS), the Institut National de la Santé et de la Recherche Médicale (INSERM), the AFM, the Université Pierre et Marie Curie-Paris 6 (UPMC), ANR (Genopath INAFIB), MyoAge (EC 7th FP, contract 223576), and the INSERM/Fiocruz and CNPq/INSERM Conjoint Programs. This article is dedicated to the memory of Ketty Schwartz, who initiated the CaPTAA network in general and particularly this project. The work was done in Paris, France. The authors declared no conflict of interest.

REFERENCES

1. Durrani, S, Konoplyannikov, M, Ashraf, M and Haider, KH (2010). Skeletal myoblasts for cardiac repair. *Regen Med* **5**: 919–932.
2. Okada, M, Payne, TR, Drowley, L, Jankowski, RJ, Momoi, N, Beckman, S *et al.* (2012). Human skeletal muscle cells with a slow adhesion rate after isolation and an enhanced stress resistance improve function of ischemic hearts. *Mol Ther* **20**: 138–145.
3. Léobon, B, Roncalli, J, Joffre, C, Mazo, M, Boisson, M, Barreau, C *et al.* (2009). Adipose-derived cardiomyogenic cells: *in vitro* expansion and functional improvement in a mouse model of myocardial infarction. *Cardiovasc Res* **83**: 757–767.
4. Ghodsizad, A, Niehaus, M, Kögler, G, Martin, U, Wernet, P, Bara, C *et al.* (2009). Transplanted human cord blood-derived unrestricted somatic stem cells improve left-ventricular function and prevent left-ventricular dilation and scar formation after acute myocardial infarction. *Heart* **95**: 27–35.
5. Ohnishi, S, Yanagawa, B, Tanaka, K, Miyahara, Y, Obata, H, Kataoka, M *et al.* (2007). Transplantation of mesenchymal stem cells attenuates myocardial injury and dysfunction in a rat model of acute myocarditis. *J Mol Cell Cardiol* **42**: 88–97.
6. Bolli, R, Chugh, AR, D'Amario, D, Loughran, JH, Stoddard, MF, Ikram, S *et al.* (2011). Cardiac stem cells in patients with ischaemic cardiomyopathy (SCIPIO): initial results of a randomised phase 1 trial. *Lancet* **378**: 1847–1857.
7. Liu, J, Zhang, Z, Liu, Y, Guo, C, Gong, Y, Yang, S *et al.* (2012). Generation, characterization, and potential therapeutic applications of cardiomyocytes from various stem cells. *Stem Cells Dev* **21**: 2095–2110.
8. Menasché, P (2012). Embryonic stem cells for severe heart failure: why and how? *J Cardiovasc Transl Res* **5**: 555–565.
9. Perez-Ilzarbe, M, Agbulut, O, Pelacho, B, Ciorba, C, San Jose-Eneriz, E, Desnos, M *et al.* (2008). Characterization of the paracrine effects of human skeletal myoblasts transplanted in infarcted myocardium. *Eur J Heart Fail* **10**: 1065–1072.
10. den Haan, MC, Grauss, RW, Smits, AM, Winter, EM, van Tuyn, J, Pijnappels, DA *et al.* (2012). Cardiomyogenic differentiation-independent improvement of cardiac function by human cardiomyocyte progenitor cell injection in ischaemic mouse hearts. *J Cell Mol Med* **16**: 1508–1521.
11. Ebelt, H, Jungblut, M, Zhang, Y, Kubin, T, Kostin, S, Technau, A *et al.* (2007). Cellular cardiomyoplasty: improvement of left ventricular function correlates with the release of cardioactive cytokines. *Stem Cells* **25**: 236–244.
12. Menasché, P, Alfieri, O, Janssens, S, McKenna, W, Reichenspurner, H, Trinquart, L *et al.* (2008). The Myoblast Autologous Grafting in Ischemic Cardiomyopathy (MAGIC) trial: first randomized placebo-controlled study of myoblast transplantation. *Circulation* **117**: 1189–1200.
13. Jiang, M, He, B, Zhang, Q, Ge, H, Zang, MH, Han, ZH *et al.* (2010). Randomized controlled trials on the therapeutic effects of adult progenitor cells for myocardial infarction: meta-analysis. *Expert Opin Biol Ther* **10**: 667–680.
14. Ohno, N, Fedak, PW, Weisel, RD, Mickle, DA, Fujii, T and Li, RK (2003). Transplantation of cryopreserved muscle cells in dilated cardiomyopathy: effects on left ventricular geometry and function. *J Thorac Cardiovasc Surg* **126**: 1537–1548.
15. Pouly, J, Hagège, AA, Vilquin, JT, Bissery, A, Rouche, A, Bruneval, P *et al.* (2004). Does the functional efficacy of skeletal myoblast transplantation extend to nonischemic cardiomyopathy? *Circulation* **110**: 1626–1631.
16. Yoo, KJ, Li, RK, Weisel, RD, Mickle, DA, Tomita, S, Ohno, N *et al.* (2002). Smooth muscle cells transplantation is better than heart cells transplantation for improvement of heart function in dilated cardiomyopathy. *Yonsei Med J* **43**: 296–303.
17. Chen, M, Fan, ZC, Liu, XJ, Deng, JL, Zhang, L, Rao, L *et al.* (2006). Effects of autologous stem cell transplantation on ventricular electrophysiology in doxorubicin-induced heart failure. *Cell Biol Int* **30**: 576–582.
18. Guarita-Souza, LC, Francisco, JC, Simeoni, R, Faria-Neto, JR and de Carvalho, KA (2011). Benefit of stem cells and skeletal myoblast cells in dilated cardiomyopathies. *World J Cardiol* **3**: 93–97.
19. Ishida, M, Tomita, S, Nakatani, T, Fukuhara, S, Hamamoto, M, Nagaya, N *et al.* (2004). Bone marrow mononuclear cell transplantation had beneficial effects on doxorubicin-induced cardiomyopathy. *J Heart Lung Transplant* **23**: 436–445.
20. Laflamme, MA, Gold, J, Xu, C, Hassanipour, M, Rosler, E, Police, S *et al.* (2005). Formation of human myocardium in the rat heart from human embryonic stem cells. *Am J Pathol* **167**: 663–671.
21. Singla, DK, Hacker, TA, Ma, L, Douglas, PS, Sullivan, R, Lyons, GE *et al.* (2006). Transplantation of embryonic stem cells into the infarcted mouse heart: formation of multiple cell types. *J Mol Cell Cardiol* **40**: 195–200.
22. Blin, G, Nury, D, Stefanovic, S, Neri, T, Guillevic, O, Brinon, B *et al.* (2010). A purified population of multipotent cardiovascular progenitors derived from primate pluripotent stem cells engrafts in postmyocardial infarcted nonhuman primates. *J Clin Invest* **120**: 1125–1139.
23. Behfar, A, Zingman, LV, Hodgson, DM, Rauzier, JM, Kane, GC, Terzic, A *et al.* (2002). Stem cell differentiation requires a paracrine pathway in the heart. *FASEB J* **16**: 1558–1566.
24. Behfar, A, Perez-Terzic, C, Faustino, RS, Arrell, DK, Hodgson, DM, Yamada, S *et al.* (2007). Cardiopoietic programming of embryonic stem cells for tumor-free heart repair. *J Exp Med* **204**: 405–420.
25. Ménard, C, Hagège, AA, Agbulut, O, Barro, M, Morichetti, MC, Brasselet, C *et al.* (2005). Transplantation of cardiac-committed mouse embryonic stem cells to infarcted sheep myocardium: a preclinical study. *Lancet* **366**: 1005–1012.
26. Laflamme, MA, Chen, KY, Naumova, AV, Muskheli, V, Fugate, JA, Dupras, SK *et al.* (2007). Cardiomyocytes derived from human embryonic stem cells in pro-survival factors enhance function of infarcted rat hearts. *Nat Biotechnol* **25**: 1015–1024.
27. Nussbaum, J, Minami, E, Laflamme, MA, Virag, JA, Ware, CB, Masino, A *et al.* (2007). Transplantation of undifferentiated murine embryonic stem cells in the heart: teratoma formation and immune response. *FASEB J* **21**: 1345–1357.
28. Arimura, T, Helbling-Leclerc, A, Massart, C, Varnous, S, Niel, F, Lacène, E *et al.* (2005). Mouse model carrying H222P-Lmna mutation develops muscular dystrophy and dilated cardiomyopathy similar to human striated muscle laminopathies. *Hum Mol Genet* **14**: 155–169.
29. Pucéat, M (2008). Protocols for cardiac differentiation of embryonic stem cells. *Methods* **45**: 168–171.
30. Pucéat, M (2007). TGFbeta in the differentiation of embryonic stem cells. *Cardiovasc Res* **74**: 256–261.
31. Yaffe, D and Saxel, O (1977). Serial passaging and differentiation of myogenic cells isolated from dystrophic mouse muscle. *Nature* **270**: 725–727.
32. Vilquin, JT, Guérette, B, Puymirat, J, Yaffe, D, Tomé, FM, Fardeau, M *et al.* (1999). Myoblast transplantations lead to the expression of the laminin alpha 2 chain in normal and dystrophic (dy/dy) mouse muscles. *Gene Ther* **6**: 792–800.
33. Simpson, EM, Linder, CC, Sargent, EE, Davisson, MT, Mobraaten, LE and Sharp, JJ (1997). Genetic variation among 129 substrains and its importance for targeted mutagenesis in mice. *Nat Genet* **16**: 19–27.
34. Swijnenburg, RJ, Schrepfer, S, Cao, F, Pearl, JI, Xie, X, Connolly, AJ *et al.* (2008). *In vivo* imaging of embryonic stem cells reveals patterns of survival and immune rejection following transplantation. *Stem Cells Dev* **17**: 1023–1029.
35. Huard, J, Roy, R, Guérette, B, Verreault, S, Tremblay, G and Tremblay, JP (1994). Human myoblast transplantation in immunodeficient and immunosuppressed mice: evidence of rejection. *Muscle Nerve* **17**: 224–234.
36. Kinoshita, I, Vilquin, JT, Guérette, B, Asselin, I, Roy, R and Tremblay, JP (1994). Very efficient myoblast allotransplantation in mice under FK506 immunosuppression. *Muscle Nerve* **17**: 1407–1415.
37. Baldwin, KM and Haddad, F (2001). Effects of different activity and inactivity paradigms on myosin heavy chain gene expression in striated muscle. *J Appl Physiol* **90**: 345–357.
38. Tezuka, A, Kawada, T, Nakazawa, M, Masui, F, Konno, S, Nitta, S *et al.* (2008). Which skeletal myoblasts and how to be transplanted for cardiac repair? *Biochem Biophys Res Commun* **369**: 270–276.
39. Charron, P, Arad, M, Arbustini, E, Basso, C, Bilinska, Z, Elliott, P *et al.*; European Society of Cardiology Working Group on Myocardial and Pericardial Diseases. (2010). Genetic counselling and testing in cardiomyopathies: a position statement of the European Society of Cardiology Working Group on Myocardial and Pericardial Diseases. *Eur Heart J* **31**: 2715–2726.
40. Wu, DC, Boyd, AS and Wood, KJ (2008). Embryonic stem cells and their differentiated derivatives have a fragile immune privilege but still represent novel targets of immune attack. *Stem Cells* **26**: 1939–1950.
41. Suzuki, K, Murtuza, B, Suzuki, N, Smolenski, RT and Yacoub, MH (2001). Intracoronary infusion of skeletal myoblasts improves cardiac function in doxorubicin-induced heart failure. *Circulation* **104**: I213–217.
42. Kirillov, AM, Fatkhudinov, TKh, Dyachkov, AV, Koroteev, AV, Goldshtein, DV and Bochkov, NP (2007). Transplantation of allogenic cells in the therapy of patients with dilated cardiomyopathy. *Bull Exp Biol Med* **144**: 635–639.

43. Leobon, B, Garcin, I, Menasche, P, Vilquin, JT, Audinat, E and Charpak, S (2003). Myoblasts transplanted into rat infarcted myocardium are functionally isolated from their host. *Proc Natl Acad Sci USA* **100**: 7808–7811.
44. Hagège, AA, Carrion, C, Menasché, P, Vilquin, JT, Duboc, D, Marolleau, JP *et al.* (2003). Viability and differentiation of autologous skeletal myoblast grafts in ischaemic cardiomyopathy. *Lancet* **361**: 491–492.
45. Chuva de Sousa Lopes, SM, Feijen, A, Korving, J, Korchynskyi, O, Larsson, J, Karlsson S *et al.* (2004). Connective tissue growth factor expression and Smad signaling during mouse heart development and myocardial infarction. *Dev Dyn* **231**: 542–550.
46. Zhao, T, Zhao, W, Chen, Y, Ahokas, RA and Sun, Y (2011). Acidic and basic fibroblast growth factors involved in cardiac angiogenesis following infarction. *Int J Cardiol* **152**: 307–313.
47. Baba, S, Heike, T, Yoshimoto, M, Umeda, K, Doi, H, Iwasa, T *et al.* (2007). Flk1(+) cardiac stem/progenitor cells derived from embryonic stem cells improve cardiac function in a dilated cardiomyopathy mouse model. *Cardiovasc Res* **76**: 119–131.
48. Yamada, S, Nelson, TJ, Crespo-Diaz, RJ, Perez-Terzic, C, Liu, XK, Miki, T *et al.* (2008). Embryonic stem cell therapy of heart failure in genetic cardiomyopathy. *Stem Cells* **26**: 2644–2653.
49. Zlatkovic-Lindor, J, Arrell, DK, Yamada, S, Nelson, TJ and Terzic, A (2010). ATP-sensitive K(+) channel-deficient dilated cardiomyopathy proteome remodeled by embryonic stem cell therapy. *Stem Cells* **28**: 1355–1367.
50. Qu, Z, Balkir, L, van Deutekom, JC, Robbins, PD, Pruchnic, R and Huard, J (1998). Development of approaches to improve cell survival in myoblast transfer therapy. *J Cell Biol* **142**: 1257–1267.
51. Habib, M, Shapira-Schweitzer, K, Caspi, O, Gepstein, A, Arbel, G, Aronson, D *et al.* (2011). A combined cell therapy and in-situ tissue-engineering approach for myocardial repair. *Biomaterials* **32**: 7514–7523.
52. Hata, H, Matsumiya, G, Miyagawa, S, Kondoh, H, Kawaguchi, N, Matsuura, N *et al.* (2006). Grafted skeletal myoblast sheets attenuate myocardial remodeling in pacing-induced canine heart failure model. *J Thorac Cardiovasc Surg* **132**: 918–924.